

Oleamide and oleamide-lipid mixed monolayers

Juan Torrent-Burgués

Department of Chemical Engineering, Universitat Politècnica de Catalunya

C/ Colom 1, 08222 Terrassa (Barcelona), Spain.

E-mail: juan.torrent@upc.edu, Tlf +34937398043, Fax +34937398225

Abstract

Oleamide (OA) and its mixtures with other lipids are of interest in some biological systems, as the tear film or the cerebrospinal fluid. In this work the behavior of OA, OA-DPPC (DPPC: dipalmitoylphosphatidylcholine) and OA-cholesterol films is studied using surface pressure-area isotherms and AFM, and analyzing the collapse pressure vs. composition, the compressibility and the mean area vs. composition for several surface pressures.

It is observed that OA forms homogeneous monolayers in a liquid expanded state until the collapse surface pressure, and that mix with DPPC and cholesterol. The collapse surface pressure changes with the mixture composition, and in the case of DPPC it is observed a noticeable influence of OA in the liquid expanded-liquid condensed (LE-LC) phase change of DPPC. The excess area is positive for the OA-DPPC films but mostly negative for the OA-cholesterol films. These results are of interest for the target of formulation of artificial tears containing lipids.

Keywords

Oleamide, Langmuir films, mixed films, tear film, AFM, π -A isotherm

Introduction

Oleamide (OA, *cis*-9-octadecenamide) is a monounsaturated lipid present in biological systems as the tear film, where is the major component of fatty amides in human Meibomian gland secretions [1]. The amount of oleamide present in the tear film is important but its function is not well known yet, but it has been proposed that it can contribute in the symptomatology of dry eye and/or ocular surface signalling [1]. Dry eye syndrome is one of the most frustrating clinical problems in daily ophthalmic practice, and artificial tears may give symptomatic relief.

OA is also present in the cerebrospinal fluid of mammal animals, transfers signals in biochemical reactions, acts as a sleep-inducing lipid and affects neurotransmission signals. OA is found in the cerebrospinal fluid of sleep-deprived cats and has been shown to induce cannabinomimetic effects including suppression of pain and inflammation. In addition, OA affects GABAergic, dopaminergic and serotonergic transmission [2]. Casford and Davies [3] also indicate that OA is a biologically and neurologically active lipid, and that it is a slip additive for polymeric and metallic friction modification. Other industrial use is as corrosion inhibitor or lubricant. Möhwald et al. [4, 5] also says that OA is an additive for medical use and food packaging in polymer products without dosage restriction and studies on the organization of OA mono and multilayers on graphite have been reported by these authors, which found a crystalline ordering in the plane of the interface when OA adsorbs on graphite. Casford and Davies [3] studied the structure of OA films at the Aluminum/Air interface by Sum Frequency Generation (SFG) Vibrational Spectroscopy and Reflection Absorption Infrared Spectroscopy (RAIRS), and found little orientational order at low compression but strong orientational order at high compression, with a perpendicular alignment of the aliphatic chain. Gu et al. [6] also suggested a perpendicular orientation of OA molecules on silver. More recent studies on OA physiological effects are [7-9].

The lipid layer of tear film, the outermost layer of the tear film, is a complex mixture of polar and neutral lipids, as triglycerides, fatty acids, diesters, cholesterol, cholesterol and wax esters, hydrocarbons and polar lipids [1, 10-14]. The lipid layer plays a major role in balancing the evaporation and isotonicity of the aqueous tear layer, and also to impart stability to the tear film and to provide a smooth optical surface for the cornea [15]. Thus the quality of the lipid layer is very important, and studies on the film-forming properties of the lipid constituents are fundamental. Between them, the polar lipid 1,2-dipalmitoyl-sn-glycero-3-phosphocholine (DPPC), that is a phospholipid, and cholesterol are significant components. The study of OA, and its mixtures with other lipids, can help in the ex-situ model of the tear film, particularly of the lipid layer. Recently, Georgiev et al. [16] studied the interactions of Meibomian gland secretion with polar lipids, as egg sphingomyelin or DPPC, in Langmuir monolayers. The studies of interactions between lipid components of the tear film may also help in the formulation of artificial tears. A former study in this direction is that of Dinslage [17] where PC and cholesterol were used to formulate a tear film substitute.

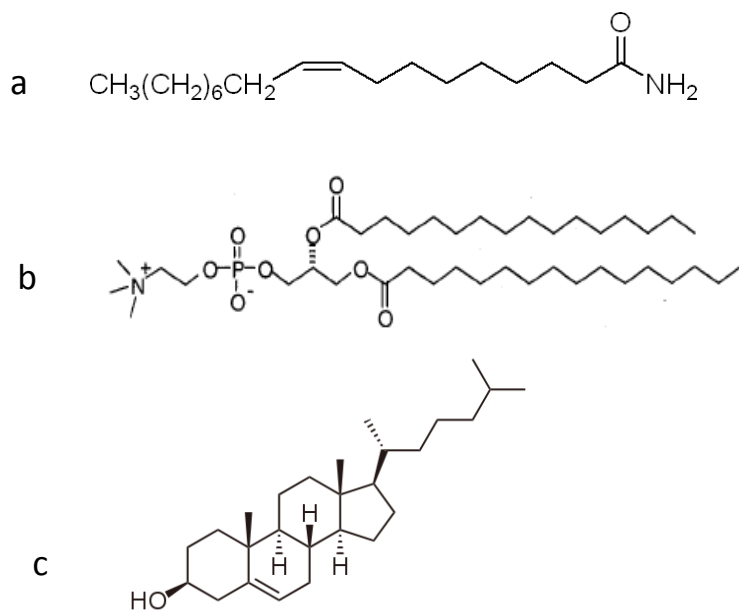
In this work the study of OA films using several subphases and mixtures with other lipids, as 1,2-dipalmitoyl-sn-glycero-3-phosphocholine (DPPC) and cholesterol (CL) is thus presented.

Experimental

Dipalmitoylphosphatidylcholine (DPPC) was purchased from Avanti Polar Lipids and cholesterol (CL) and oleamide (OA) (see scheme 1) were from Sigma-Aldrich. KH_2PO_4 , NaCl and chloroform of analytical grade were used in solutions preparation. Water was ultrapure MilliQ (18.2 $\text{M}\Omega\cdot\text{cm}$). Mica sheets were purchased to TED PELLA Inc (CA). Langmuir and Langmuir-Blodgett (LB) monolayer formation were carried on a Nima model 1232D1D2 trough and using MilliQ® quality water as subphase. Solutions of OA, DPPC, CL, DPPC:OA and CL:OA were prepared using chloroform. LB monolayers were transferred to the corresponding substrate surface at defined surface pressures

values. Barrier closing rates were fixed at $50 \text{ cm}^2 \cdot \text{min}^{-1}$ ($2.5 \text{ cm} \cdot \text{min}^{-1}$) for isotherm registration and at $25 \text{ cm}^2 \cdot \text{min}^{-1}$ ($1.25 \text{ cm} \cdot \text{min}^{-1}$) for LB film transfer. No noticeable influence of these compression rates was observed on the isotherm shape. Isotherm recording is carried out adding the solution to the subphase and waiting 15 minutes for perfect spreading. The isotherms were repeat three times to ensure reproducibility. LB film transfer was conducted dipping the substrate (mica sheet) on the subphase before spreading the solution and five minutes were lagged after surface pressure setpoint was achieved. Transfer speed was set at 5 mm/min linear velocity. Experiments were conducted at 22°C .

The AFM topographic images of LB films were acquired in tapping mode using a Multimode AFM controlled by a Nanoscope IV electronics (Veeco, Santa Barbara, CA). Silicon tips with a nominal spring constant of $40 \text{ nN} \cdot \text{nm}^{-1}$ were used (ACT-W, Applied Nanostructures, Santa Clara, CA). Images were acquired at 1.5 Hz and at minimum vertical force so as to reduce sample damage.



Scheme 1 Molecular structures of: a) oleamide (OA), cis-9-octadecenamide, b) 1,2-dipalmitoyl-sn-glycero-3-phosphocholine (DPPC), c) Cholesterol (CL)

Results and discussion

- Individual components

Films at the air-water interphase were obtained for the individual components OA, CL and DPPC, which were also transferred onto mica for AFM observation. The surface pressure-area (π -A) isotherms of OA on water (Figure 1), saline solution and phosphate buffered saline solution were registered. No influence of these ionic subphases has been observed in the π -A isotherms (Figure 2), and no noticeable influence of the compression velocity is observed. The isotherm shape shows that after reaching a maximum surface pressure, a plateau is followed corresponding to a multilayer formation (with very low values of the area per molecule). The isotherm cycle (Figure 1) also shows a quasi reversible behaviour when decompressing, with the decompressing isotherm tending to the shape and position of the compressing isotherm. Further compressions follow the original isotherm, confirming the reversibility.

AFM images (see Figures 5 and 6) show a uniform film at the different surface pressures (4 and 22 mN/m, respectively). The AFM images do not show the interesting structures observed by Möhwald et al. [4, 5] using spin coating for deposition of OA on highly orientated pyrolytic graphite, allowing to conclude that the deposition technique and the substrate play an important role in the organization of OA molecules. The compressibility coefficient ($\beta = -1/A(\delta A/\delta \pi)_T$) values from the isotherm (0.014 m \cdot mN $^{-1}$ at $\pi = 15$ mN \cdot m $^{-1}$ and Table 1), as well as AFM images, point to a liquid expanded, LE, phase.

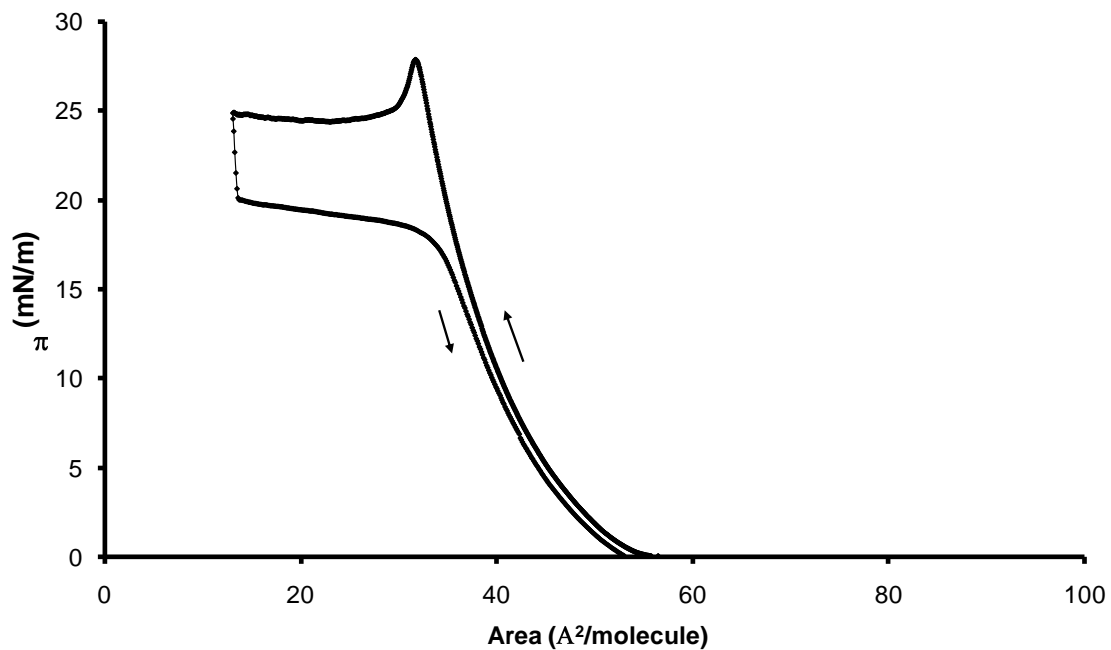


Figure 1 π -A isotherm cycle for OA on water

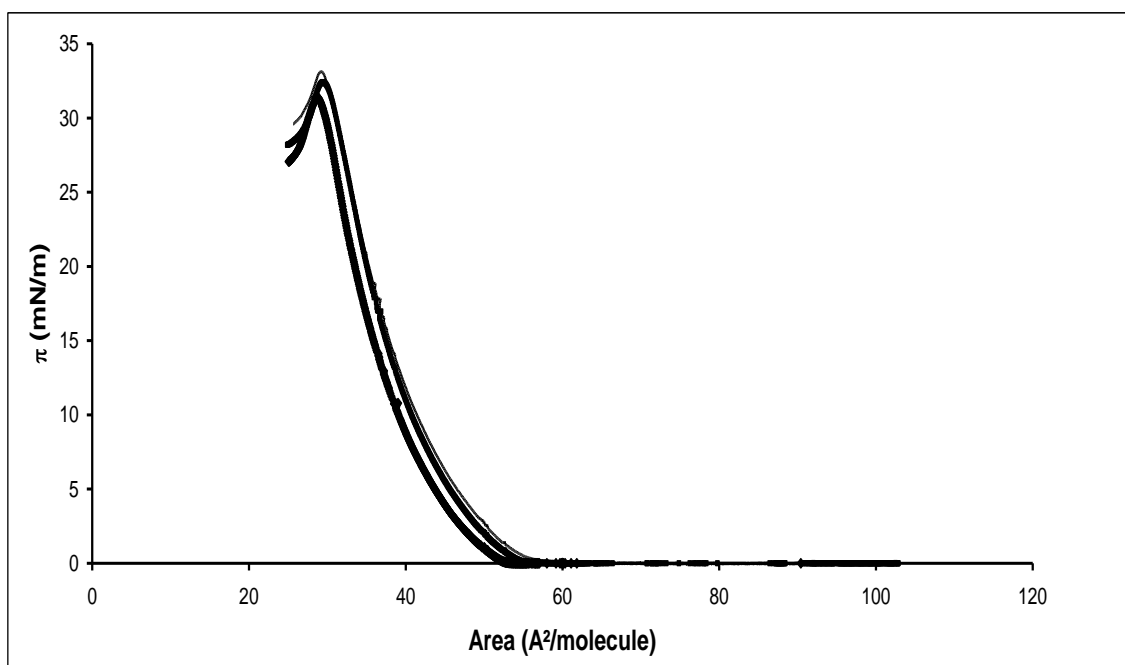


Figure 2 π -A isotherms for OA on: water (thick line), 0.9% NaCl (medium line), 0.9%NaCl+phosphate buffer pH=7.4 (thin line)

The isotherms of DPPC are very similar at the three subphases, thus no influence of these ionic subphases has been observed. In figure 3 the isotherm of DPPC on water can be observed, showing the characteristic phase change from liquid expanded (LE) to liquid condensed (LC) state with a large plateau at π ca 6-7 $\text{mN}\cdot\text{m}^{-1}$. The compressibility equals 0.032 $\text{m}\cdot\text{mN}^{-1}$ (LE) at $\pi=4$ $\text{mN}\cdot\text{m}^{-1}$ and 0.0051 $\text{m}\cdot\text{mN}^{-1}$ (LC) at $\pi=25$ $\text{mN}\cdot\text{m}^{-1}$ (for more values see Table 1).

In figure 7 the isotherm of CL on water can be observed. The isotherms of CL are also similar at the three subphases, showing a slope change at ca 10 $\text{mN}\cdot\text{m}^{-1}$, and compressibility values indicate a LC state at π below 10 $\text{mN}\cdot\text{m}^{-1}$ and a solid state (S) at π above 10 $\text{mN}\cdot\text{m}^{-1}$. The compressibility equals 0.0043 $\text{m}\cdot\text{mN}^{-1}$ (LC) at $\pi=5$ $\text{mN}\cdot\text{m}^{-1}$ and 0.0019 $\text{m}\cdot\text{mN}^{-1}$ (S) at $\pi=25$ $\text{mN}\cdot\text{m}^{-1}$ (for more values see Table 2). On the other hand, no noticeable influence of the compression velocity is observed.

AFM images of DPPC or CL monolayers are presented in the next section when compared with those of mixed films.

- **Mixed films**

π -A isotherms of mixtures of OA with DPPC or CL, Area vs composition plots, and AFM images, permit to characterize the behaviour of OA mixed with these other lipids usually present in biological systems.

Surface pressure-Mean Area isotherms of mixtures of OA with DPPC are plotted in Figure 3a. It is seen, on one hand, a notable influence of OA on the phase change of the DPPC isotherm, and, on the other hand, the collapse pressure, π_c , changes accordingly with the composition (Figure 3b). These facts indicate an interaction between both components and miscibility. In this case (DPPC-OA) the π_c decreases when the proportion of OA increases. The plots of the mean area vs. composition (Figure 4) indicate positive deviations from the ideal behavior (that means that the

excess area $A^E = A - A^{id} = A - (\sum X_i A_i) > 0$) at all the analyzed surface pressures and at all compositions, but especially for the lowest DPPC molar fraction ($X(\text{DPPC}) = 0.154$). This result is significant since Georgiev et al. [12] found that in a pseudo-mixture of Meibomian gland secretion (MGS) with DPPC the Area deviates negative values from ideality, in an opposite sense to the results reported for OA. Since the MGS is a complex mixture of lipids, it is clear that others substances than OA are responsible for that behavior.

Compressibility coefficient values for the DPPC:OA mixtures (Table 1) are, in general, bigger than those of DPPC and more similar to those of OA, much more similar when the OA content increases. These values corresponds to a LE state, but very close to a LC state for mixtures of high DPPC content and at high surface pressures.

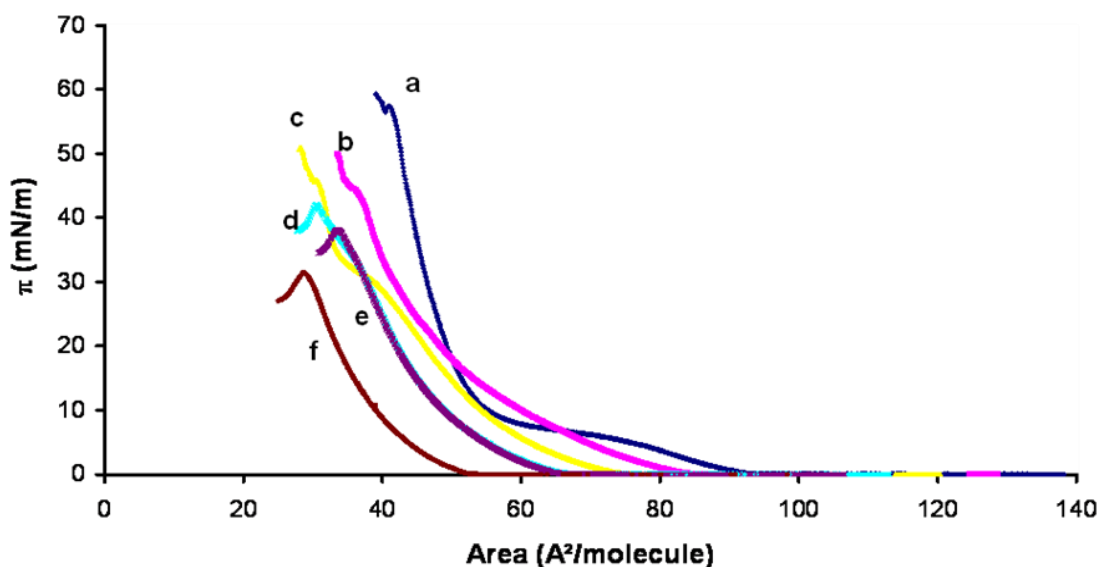


Figure 3a Surface pressure-Mean Area isotherms for DPPC-OA, $X(\text{DPPC})$: 1 (DPPC) blue (a), 0.745 magenta (b), 0.522 yellow (c), 0.327 cyan (d), 0.154 violet (e), 0 (OA) brown (f)

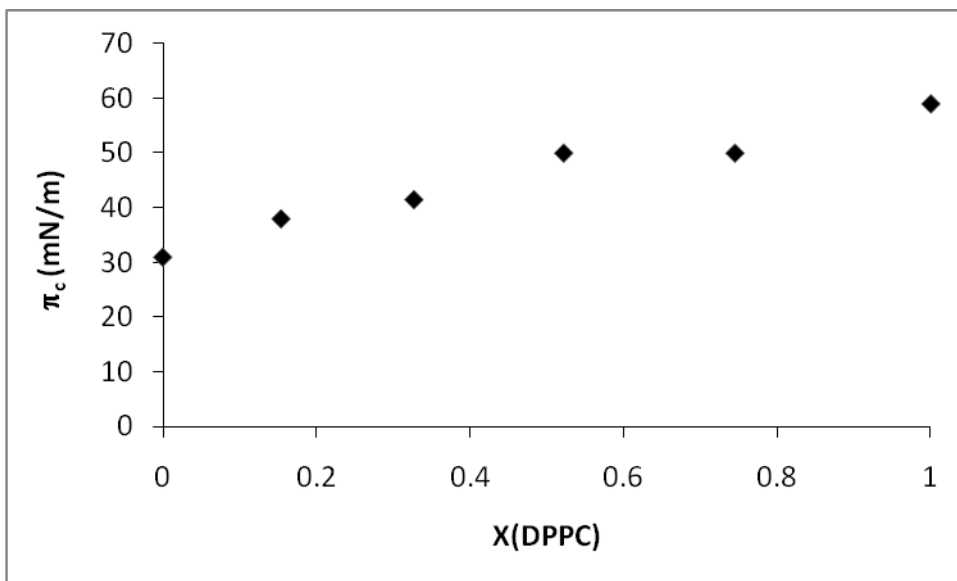


Figure 3b Collapse pressure π_c vs. X(DPPC) for DPPC-OA mixed films

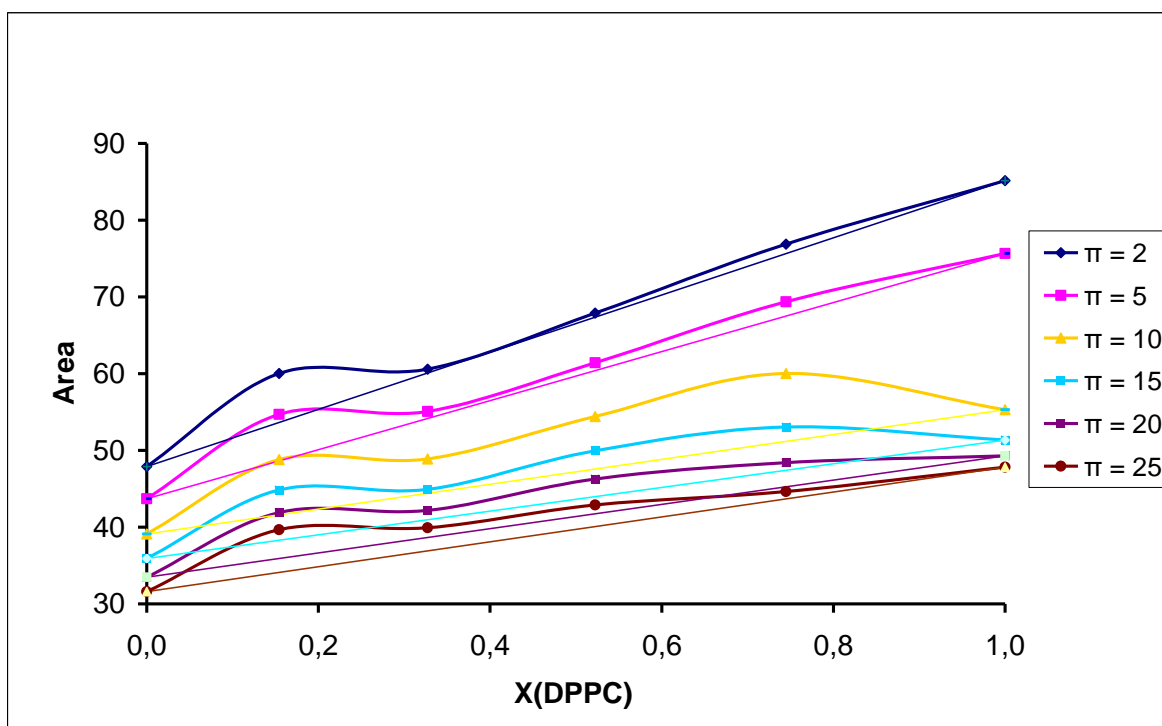


Figure 4 Mean Area vs. composition for DPPC-OA at several surface pressures ($\pi=2, 5, 10, 15, 20, 25$ mN·m⁻¹). Straight lines represent the ideal behavior

Table 1. Compressibility coefficients of DPPC:OA mixtures at several surface pressures.

π (mN/m)	$X_{\text{DPPC}}=1$	$X_{\text{DPPC}}=0.745$	$X_{\text{DPPC}}=0.522$	$X_{\text{DPPC}}=0.327$	$X_{\text{DPPC}}=0.154$	$X_{\text{DPPC}}=0$
5	0.032	0.028	0.046	0.037	0.027	0.028
10	0.017	0.028	0.020	0.022	0.020	0.019
15	0.0084	0.022	0.015	0.015	0.014	0.014
20	0.0070	0.016	0.014	0.012	0.012	0.012
25	0.0051	0.015	0.015	0.012	0.0106	0.0095
30	0.0053	0.013	0.028	0.012	0.0111	
35	0.0043	0.0092	0.014	0.019	0.0131	
40	0.0051	0.0066	0.0052	0.019		

AFM images of LB films of several DPPC:OA mixtures when compared with those of the pure components (Figures 5 and 6) also show the influence of OA on the DPPC phase change. Figure 5A shows the two phases LE and LC of DPPC at low surface pressures, meanwhile Figures 5B and 5C show that OA difficult this phase change, appearing the DPPC LC domains more fragmented. In particular, at the lower DPPC molar fraction, that corresponds to the greater deviation in the Area from ideality (Figure 4), the domains are big but separated by high distances, predominating the fluid phase. This fluid phase corresponds to OA, or is rich in OA, meanwhile the domains corresponds to DPPC, or are rich in DPPC. At higher surface pressures (Figure 6), the LC phase appears predominant for the higher DPPC molar fraction, but still very fragmented for the lower DPPC molar fraction. These observations are in agreement with the analysis of the area composition plots. The presence of OA difficult the interactions between DPPC molecules which tend to compact them to a more condensed state. The height of the condensed domains in respect to the LE phase in Figures 5a (DPPC) and 5b (high DPPC content) is the same, 0.8 nm, being of 1.1 nm in Figure 5c due to the low DPPC content. The domain height at a higher surface pressure in Figure 6b (high DPPC content) is 0.3-0.4 nm, being of 0.6 nm in Figure 6c due to the low DPPC content. On the other hand, at the same surface pressure, the % of domain surface coverage decreases with the presence of OA. At high surface pressure this % is close to that of the DPPC fraction in the mixture but it is always lower (at $\pi=22$ mN/m these %, calculated over several images, are around 55 and 11 for X_{DPPC} of 0.74 and 0.15,

respectively), fact that indicates that some DPPC remains in the LE phase mixed with OA.

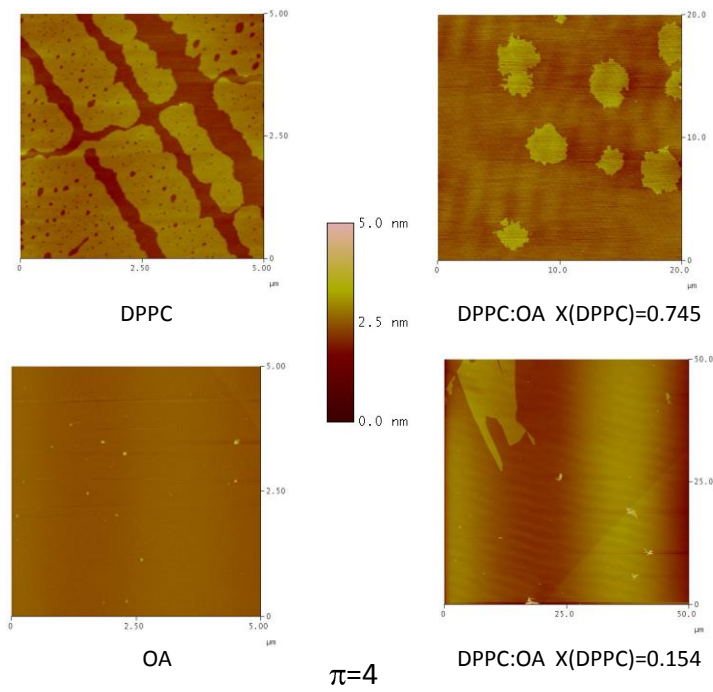


Figure 5 AFM images of pure DPPC, pure OA, and mixed DPPC:OA at $\pi=4 \text{ mN}\cdot\text{m}^{-1}$

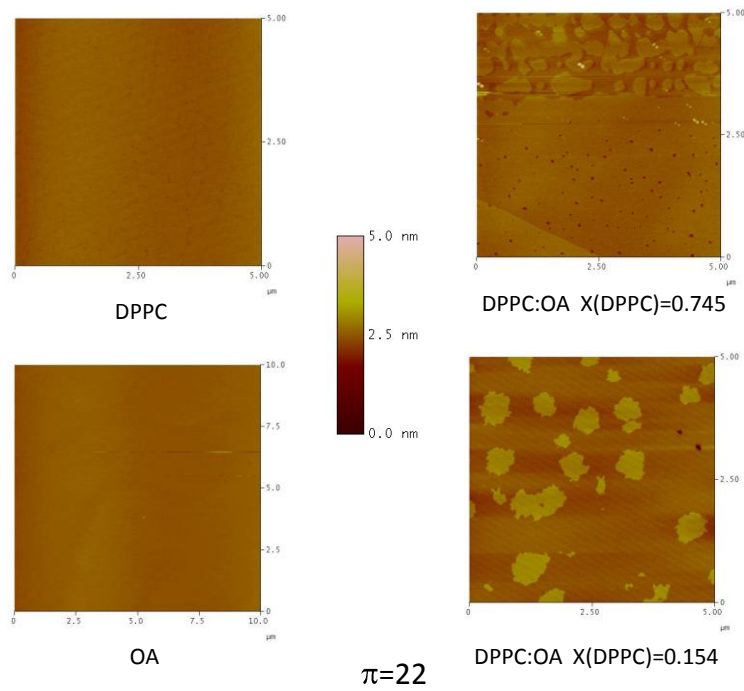


Figure 6 AFM images of pure DPPC, pure OA, and mixed DPPC:OA at $\pi=22 \text{ mN}\cdot\text{m}^{-1}$

Surface pressure-Mean Area isotherms of mixtures of OA with CL are plotted in Figure 7a. It is seen that the collapse pressure change with composition, indicating mixing (Figure 7b). In this case the π_c first increases and after decreases when the proportion of OA increases, going through a maximum. This maximum is not observed for DPPC:OA mixtures. The plots of the mean area vs. composition (Figure 8) indicate negative deviations from the ideal behavior at all the analyzed surface pressures and compositions except for the higher OA molar fraction, where these deviations become positives. A minimum is presented at $X(\text{OA})=0.574$ and a maximum at $X(\text{OA})=0.924$. The minimum in mean area vs. composition is close to the maximum in π_c vs. composition, indicating that OA:CL mixtures with a molar composition around 1:1 are more stable and that perhaps some kind of complex forms between OA and CL molecules, probably through the NH_2 and OH groups.

Compressibility coefficient values for the OA:CL mixtures (Table 2) are between those of OA and those of CL, varying with the composition; more OA in the mixture more similar to pure OA. The state of the mixed films changes from LE to LC with increasing the CL content.

AFM images at several compositions and surface pressures show uniform films with no phase separation. Figure 9 shows that for a surface pressure of $5 \text{ mN}\cdot\text{m}^{-1}$, but images at $22 \text{ mN}\cdot\text{m}^{-1}$ (not shown) present the same characteristics. Thus, these data indicate mixing between OA and CL with favourable interactions at practically all of the studied conditions.

Future research will be addressed to observe and analyze the interactions of OA with other tear film lipids and with the Meibomian gland secretion.

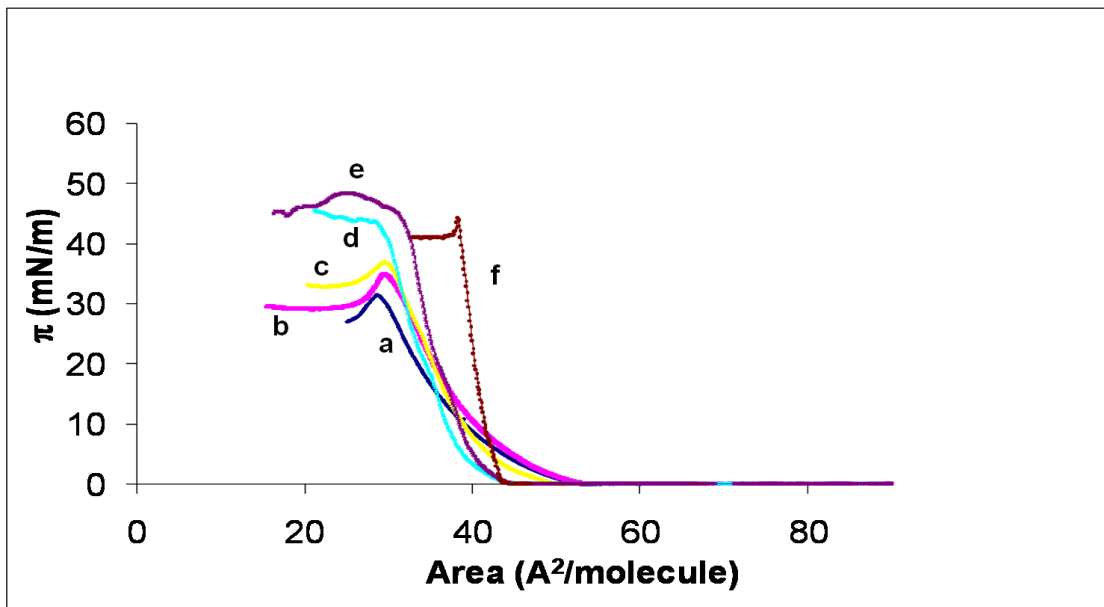


Figure 7a Surface pressure-Mean Area isotherms for OA-CL monolayers on water. X(OA): 1 (OA) blue (a), 0.924 magenta (b), 0.802 yellow (c), 0.574 cyan (d), 0.473 violet (e), 0 (CL) brown (f)

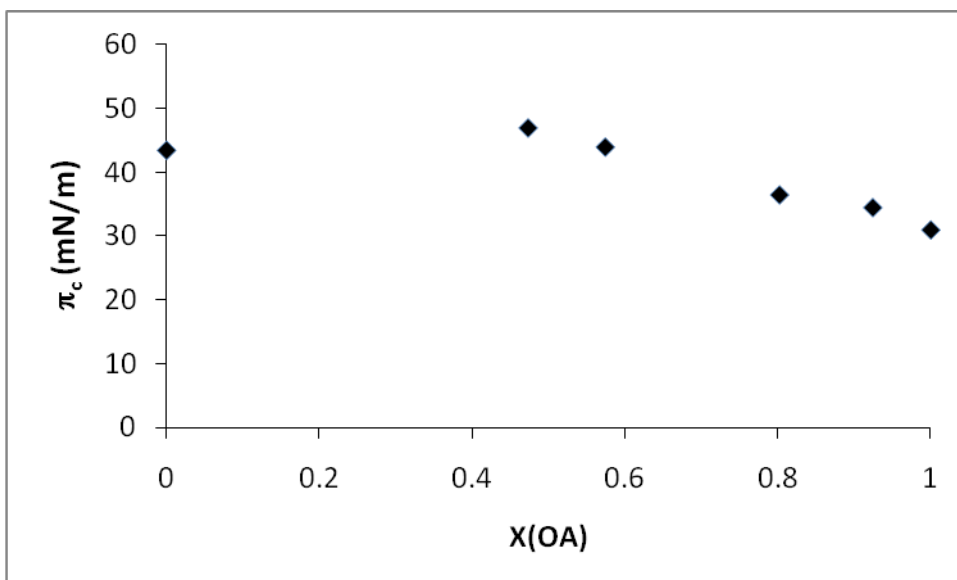


Figure 7b Collapse pressure π_c vs. X(OA) for OA-CL mixed films

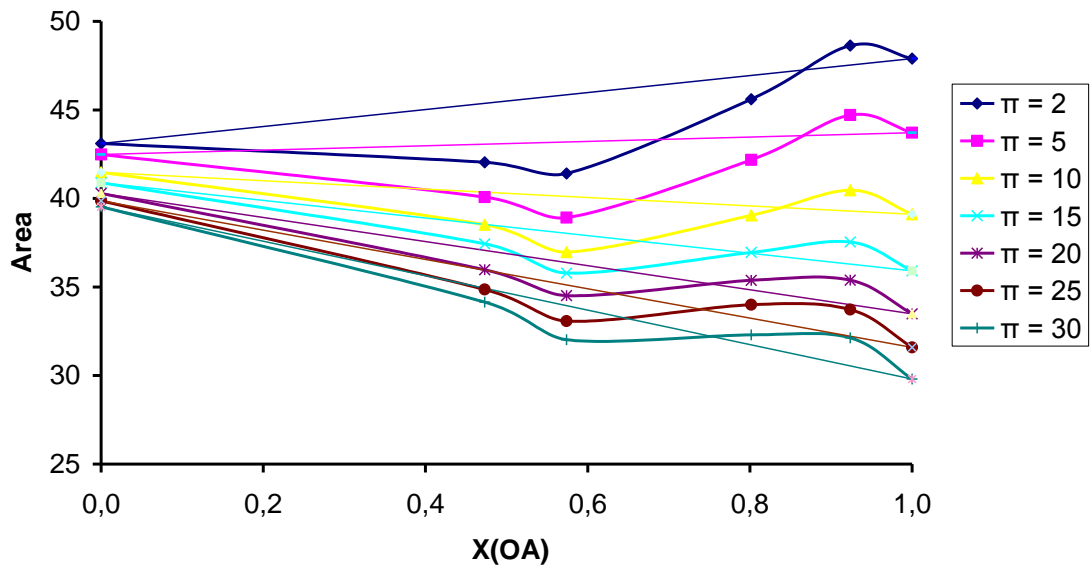


Figure 8 Mean area vs. composition for OA-CL mixtures at several surface pressures ($\pi=2, 5, 10, 15, 20, 25, 30 \text{ mN} \cdot \text{m}^{-1}$). Straight lines represent the ideal behavior

Table 2. Compressibility coefficients of OA:CL mixtures at several surface pressures.

π (mN/m)	$X_{OA}=1$	$X_{OA}=0.924$	$X_{OA}=0.802$	$X_{OA}=0.574$	$X_{OA}=0.473$	$X_{OA}=0$
5	0.028	0.024	0.019	0.014	0.0114	0.0043
10	0.019	0.017	0.013	0.0076	0.0060	0.0031
15	0.014	0.013	0.0093	0.0059	0.0059	0.0025
20	0.012	0.0107	0.0077	0.0097	0.0081	0.0024
25	0.0095	0.0097	0.0095	0.0069	0.0047	0.0017
30		0.0111	0.0098	0.0052	0.0039	0.0019
35			0.0105	0.0053	0.0039	0.0019
40				0.0090	0.0049	0.0020

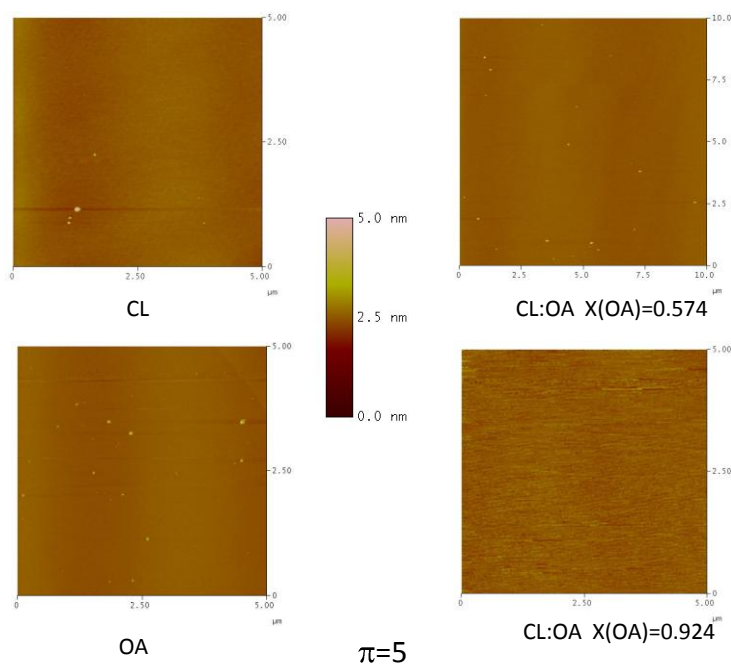


Figure 9 AFM images of pure CL, pure OA, and mixed CL:OA at $\pi=5 \text{ mN}\cdot\text{m}^{-1}$

Conclusions

OA form stable and homogeneous monolayers with a relatively low surface pressure collapse, in accordance with the analogue unsaturated fatty acid oleic acid.

The analysis of isotherms, Area vs. composition plots and AFM images at several π and compositions show mixing between DPPC and OA and between CL and OA, but with less favourable interactions at most of the studied conditions for DPPC:OA. AFM images of DPPC and DPPC:OA mixtures show the presence of domains of the LC phase, and the morphology of these domains depend on the surface pressure but also on the OA content. This can be attributed to the effect of OA molecules on the DPPC molecules that difficult the DPPC phase change from the LE to the LC state.

As OA is the major component of fatty amides in human Meibomian gland secretions, the results here presented, and complemented with future research with other tear

film lipids, can help in understanding the behaviour of the tear film and its problems and solutions.

Acknowledgement

The author thanks the economical support of the Spanish Government through the project CTQ2007-68101-C02-02.

References

- [1] Nichols KK, Ham BM, Nichols JJ, Ziegler C, Green-Church KB (2007). Invest. Ophthalmol. Vis. Sci. 48: 34-39.
- [2] Walker JM, Krey JF, Chu C J, Huang SM (2002). Chem. Phys. Lipids 121: 159-172.
- [3] Casford MTL, Davies PB (2009). Appl. Mater. & Interf. 1: 1672-1681.
- [4] Miyashita N, Möhwald H, Kurth DG (2007). Chem. Mater. 19: 4259-4262.
- [5] Zhang R, Möhwald H, Kurth DG (2009). Langmuir 25: 2290-2293.
- [6] Gu YJ, Shi ZM, Nie CS (1998). Appl. Spectrosc. 52: 855-862.
- [7] Soria-Gómez E, Márquez-Diosdado MI, Montes-Rodríguez CJ, Estrada-González V, Prospéro-García O (2010). J Neuropsychopharmacol. 13: 1247-1254.
- [8] Oh YT, Lee JY, Lee J, Lee JH, Kim JE, Ha J, Kang I (2010). Neurosci Lett. 474: 148-53.
- [9] Sudhakar V, Shaw S, Imig JD (2009). Eur J Pharmacol. 607: 143-50.
- [10] McCulley JP, Shine WE (2001). Biosci. Rep. 21: 407-418.
- [11] Butovich IA (2009). Prog. Retinal Eye Res. 28: 483-498.

- [12] Butovich IA (2008). *Invest. Ophthalmol. Vis. Sci.* 49: 3779-3789.
- [13] Butovich IA, Uchiyama E, Di Pascuale MA, McCulley JP (2007). *Lipids* 42: 765-776.
- [14] Borchman D, Foulks GN, Yappert MC, Tang D, Ho DV (2007). *Chem. Phys. Lipids* 147: 87-102.
- [15] Bron AJ, Tiffany JM, Gouveia SM, Yokoi N, Voon LW (2004). *Exp. Eye Res.* 78: 347-360.
- [16] Georgiev GA, Kutsarova E, Jordanova A, Krastev R, Lalchev Z (2010). *Colloids Surf. B* 78: 317-327.
- [17] S Dinslage, W Stoffel, M Diestelhorst, G Krieglstein (2002). *Cornea* 21: 352-355.

Caption Figures

Scheme 1 Molecular structures of: a) oleamide (OA), cis-9-octadecenamide, b) 1,2-dipalmitoyl-sn-glycero-3-phosphocholine (DPPC), c) Cholesterol (CL)

Figure 1 π -A isotherm cycle for OA on water

Figure 2 π -A isotherms for OA on: water (thick line), 0.9% NaCl (medium line), 0.9%NaCl+phosphate buffer pH=7.4 (thin line)

Figure 3a Surface pressure-Mean Area isotherms for DPPC-OA, X(DPPC): 1 (DPPC) blue (a), 0.745 magenta (b), 0.522 yellow (c), 0.327 cyan (d), 0.154 violet (e), 0 (OA) brown (f)

Figure 3b Collapse pressure π_c vs. X(DPPC) for DPPC-OA mixed films

Figure 4 Mean Area vs. composition for DPPC-OA at several surface pressures ($\pi=2, 5, 10, 15, 20, 25 \text{ mN}\cdot\text{m}^{-1}$). Straight lines represent the ideal behavior

Figure 5 AFM images of pure DPPC, pure OA, and mixed DPPC:OA at $\pi=4 \text{ mN}\cdot\text{m}^{-1}$

Figure 6 AFM images of pure DPPC, pure OA, and mixed DPPC:OA at $\pi=22 \text{ mN}\cdot\text{m}^{-1}$

Figure 7a Surface pressure-Mean Area isotherms for OA-CL monolayers on water. X(OA): 1 (OA) blue (a), 0.924 magenta (b), 0.802 yellow (c), 0.574 cyan (d), 0.473 violet (e), 0 (CL) brown (f)

Figure 7b Collapse pressure π_c vs. X(OA) for OA-CL mixed films

Figure 8 Mean area vs. composition for OA-CL mixtures at several surface pressures ($\pi=2, 5, 10, 15, 20, 25, 30 \text{ mN}\cdot\text{m}^{-1}$). Straight lines represent the ideal behavior

Figure 9 AFM images of pure CL, pure OA, and mixed CL:OA at $\pi=5 \text{ mN}\cdot\text{m}^{-1}$